Toxicology Reports 14 (2025) 102041

Contents lists available at ScienceDirect

Toxicology Reports

journal homepage: www.elsevier.com/locate/toxrep

Chlorpyrifos abolished C2C12 myoblast cell proliferation and differentiation via mitochondrial stress

Piyaporn Surinlert [a,b], Laksika Petmunee [c], Chatchakwan Jiraarpassorn [c], Thanaporn Salika [c], Mariam Watthanard [c], Kornkanok Bunnuang [d], Thanvarin Thitiphatphuvanon [e], Tanaporn Hengpratom [d], Chittipong Tipbunjong [d,*]

[a] Chulabhorn International College of Medicine, Thammasat University, Pathum-Thani 12120, Thailand
[b] Thammasat University Research Unit in Synthesis and Applications of Graphene, Thammasat University, Pathum-Thani 12120, Thailand
[c] Hatyaiwittayalai School, Songkhla 90110, Thailand
[d] Division of Health and Applied Sciences, Faculty of Science, Prince of Songkla University, Songkhla 90110, Thailand
[e] Faculty of Medicine, Kasetsart University, Bangkok 10900, Thailand

ARTICLE INFO

Handling Editor: Prof. L.H. Lash

Keywords:
Chlorpyrifos
C2C12 Myoblasts
Proliferation
Differentiation
Reactive Oxygen Species
Myosin Heavy Chain
Myogenesis
Skeletal Muscle

ABSTRACT

Background: Chlorpyrifos (CPF) is a widely used organophosphate insecticide reported to contaminate agricultural products, and is absorbed through the gastrointestinal mucosa, respiratory epithelium, and skin. To date, knowledge about the effect of CPF on skeletal muscle stem cells responsible for muscle formation and regeneration is still limited. Hence, this study aimed to investigate the effects of CPF on skeletal muscle stem cell proliferation, differentiation, and mitochondrial stress.

Methods: This study used the C2C12 myoblast cell line as a model for skeletal muscle stem cells. The myoblasts were treated with CPF at 0–100 μM for 24–72 h. Cell viability and proliferation were determined by MTT assay, cell counting, Ki-67 immunostaining, and flow cytometry. Reactive oxygen species (ROS) production was determined by H_2DCFDA assay, and mitochondrial stress-related gene expression determined by real-time polymerase chain reaction. Differentiated myotube formation was measured by immunostaining and western blotting.

Results: Treatment with 50–100 μM CPF significantly decreased myoblast cell viability and cell proliferation 24 h after treatment. Flow cytometry revealed that CPF significantly decreased cells in G0/G1, but increased cell accumulation at Sub G0/G1, S, and G2/M cell cycle phases. In addition, CPF significantly increased ROS production and downregulated mitochondrial-related genes *OPA-1*, *Mfn-1*, *Mfn-2*, and *Pink-1*, but upregulated *Cyt-c* expression leading to caspase-3 activation. Moreover, 10–25 μM CPF significantly diminished myoblast differentiation by decreasing both the number and size of multinucleated myotubes. The myoblast differentiation markers myosin heavy chain and myogenin (but not MyoD) also decreased with CPF treatment. A possible mechanism of myoblast proliferation and differentiation inhibition by CPF may occur through inhibition of Akt phosphorylation.

Conclusion: CPF potentially abrogated myoblast proliferation and differentiation by inhibiting Akt phosphorylation. These findings raise concerns about the potential adverse effects of CPF contamination in agricultural products on consumers.

1. Introduction

Pesticides are substances used for repelling and killing insects in agricultural settings worldwide. The widespread application of pesticides exposes human health to these toxic products [1]. There are a range of broad-spectrum pesticides currently in use, one of which is Chlorpyrifos (CPF). CPF (O,O-diethyl O-(3,5,6-trichloro-2-pyridinyl)-phosphorothioate (Fig. 1), also known as chlorpyrifos ethyl, is an organophosphate which causes toxicity by inhibiting acetylcholinesterase (AChE), an enzyme which hydrolyses acetylcholine at cholinergic synapses. CPF is used worldwide for insect control in a range of crops [2,3]. However, it causes toxicity not only in the target

* Corresponding author.
E-mail address: chittipong.t@psu.ac.th (C. Tipbunjong).

https://doi.org/10.1016/j.toxrep.2025.102041
Received 12 February 2025; Received in revised form 12 April 2025; Accepted 24 April 2025
Available online 28 April 2025

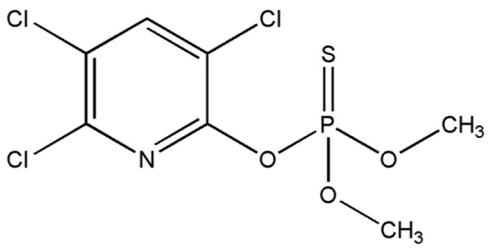

Fig. 1. Chemical structure of Chlorpyrifos (CPF).

insect species, but also in non-insect species such as humans.

CPF has been reported to enter the bloodstream via gastrointestinal mucosa absorption, and can also be absorbed through the respiratory epithelium and skin [4,5]. In the respiratory tract, it targets the alveoli, which perform a gas exchange function in humans and other animals [6]. Dermal absorption of CPF has been shown to produce toxicity in animal studies [7,8]. Upon entering the body, CPF stimulates the inhibition of AChE, cellular oxidative stress, and endocrine disruption [9]. Several studies have demonstrated the effect of CPF on skeletal muscle through decreased AChE activity and contractile performance in diaphragmatic muscle. CPF also affects myosin heavy chain (MHC) isoform expression by decreasing the MHC I isoform and increasing the fast-twitch MHC IIa isoform [10].

Skeletal muscle is the largest tissue in the human body responsible for movement and metabolism. During embryonic development, myoblasts differentiate into myocytes and fuse together to form multinucleated myofibres under the regulation of paired box (Pax: Pax7 and Pax3) and myogenic regulatory factors (MRFs: MyoD, Myf5, myogenin, and MRF4) [11]. However, several cells do not fuse to form myofibres, but reside within the basement membrane of the associated myofibre, called satellite cells. These are adult skeletal muscle stem cells which are activated and enter cell division and differentiation to repair injured muscle fibres or form new muscle fibres [12]. Disruption of myogenesis may cause incomplete muscle regeneration and repair. There are numerous contaminant chemicals which have been reported to delay or even abolish myogenesis, such as bisphenol-A [13], styrene oxide [14], arsenic [15], paraquat [16], and others. To date, knowledge about the effect of CPF on skeletal muscle cell growth and development is still limited. The objective of this study was to investigate the effects of CPF on muscle cell proliferation, differentiation, and stress, as well as the underlying mechanism.

2. Materials and methods

2.1. Chemicals and reagents

Unless otherwise indicated, chemicals and reagents for cell culture experiments were purchased from Gibco (Massachusetts, USA). Basic chemicals for molecular investigations and 3-(4,5-dimethylthiazol-2-yl)-2,5-diphenyltetrazolium bromide (MTT) were from Sigma-Aldrich (Missouri, USA). CPF was purchased from Supelco (Darmstadt, Germany), and 2′,7′-dichlorodihydrofluorescein diacetate (H_2DCFDA) was purchased from Invitrogen (Massachusetts, USA). Luna Universal qPCR Master Mix real-time polymerase chain reaction (PCR) reagent was obtained from New England Biolabs (Massachusetts, USA). Primary antibodies, including mouse monoclonal anti-MHC, mouse monoclonal anti-myogenin, mouse monoclonal anti-MyoD, mouse monoclonal anti-Bcl-2, mouse monoclonal anti-tubulin, and secondary antibodies were purchased from Merck Millipore (Massachusetts, USA). Rabbit monoclonal anti-caspase-3, rabbit monoclonal anti-Cyt-c, mouse monoclonal anti-phospho-Akt, rabbit monoclonal anti-Akt, rabbit monoclonal anti-phospho-ERK, rabbit monoclonal anti-ERK, rabbit monoclonal anti-phospho-p38, and rabbit monoclonal anti-p38 antibodies were purchased from Cell Signaling Technology (Massachusetts, USA). Hoechst 33342 and DAPI were purchased from Abcam (Cambridge, UK). Enhanced chemiluminescence detection reagent was obtained from Cytiva (Amersham, UK).

2.2. Cell culture and treatment

The C2C12 mouse myoblast cell line was purchased from American Type Culture Collection (ATCC, Manassas, Virginia, USA), and was maintained in growth medium (GM) composed of DMEM supplemented with 10 % foetal bovine serum and 1 % antibiotics at 37 °C in a humidified CO_2 incubator set to 5 % CO_2. The myoblast cells were subcultured when they reached 70 % confluence, seeded into cell culture plates, and allowed to attach and grow overnight.

For the cytotoxicity assay, the cells were treated with various concentrations of CPF for 24–72 h in low-serum media before being photographed and undergoing an MTT assay.

For cell proliferation and cell stress assays, cells were treated with various concentrations of CPF in GM for 24–72 h before being photographed and undergoing an MTT assay, flow cytometry, real-time PCR, and a H_2DCFDA assay.

To evaluate differentiation, confluent cells were shifted to a differentiation media (DM) composed of DMEM supplemented with 2 % horse serum in the presence of CPF at indicated concentrations for 72 h before undergoing immunofluorescence staining and western blotting.

2.3. MTT assay

The treated cells were incubated with 0.5 mg/ml MTT diluted in GM for 3 h at 37 °C in a CO_2 incubator. The MTT mixture was then discarded and replaced with dimethyl sulfoxide. After constant agitation, the absorbance was measured at 570 nm with a microplate reader (BioTek Synergy HT).

2.4. Cell count

The treated cells were trypsinised and centrifuged. The pellet was resuspended in phosphate buffered saline (PBS) and cell number determined using a haemocytometer under a light microscope. Trypan blue exclusion was used to determine the number of viable and dead cells.

2.5. Flow cytometry

The treated cells were trypsinised and centrifuged to collect the pellet. The pellet was resuspended in PBS and fixed with ice-cold 70 % ethanol for 10 min. After several washes with PBS, the pellet was incubated with RNase A at 37 °C and stained with propidium iodide. Cell cycle distribution was determined using a Becton Dickinson flow cytometer (BD Bioscience).

2.6. Reactive oxygen species (ROS) assay

The treated cells were incubated with H_2DCFDA diluted in GM for 30 min. After incubation, the cells were washed and incubated with Hoechst 33342 for live-cell nuclear staining. The ROS activity was detected using fluorescence microscopy (Olympus IX73) at 488 nm excitation wavelength and 520 nm emission filter for green fluorescent signal. The nucleus was detected at 350 nm excitation wavelength and 460 nm emission filter for blue fluorescent signal. The fluorescence intensity was measured using ImageJ software (version 1.8.0).

2.7. Immunofluorescence staining

The treated cells were fixed with 4 % paraformaldehyde for 20 min. After several washes and rehydration with PBS, the cells were permeabilised with 0.3 % Triton X-100 in PBS for 30 min. The cells were

blocked with 5 % goat serum in PBS for 1 h before incubation with anti-MHC antibody overnight at 4 °C. After several washings, the cells were incubated with secondary antibody conjugated with Alexa Fluor 488 goat anti-mouse IgG (488 nm excitation wavelength/520 nm emission filter for green fluorescent signal) or Alexa Fluor 568 goat anti-rabbit IgG (568 nm excitation wavelength/620 nm emission filter for red fluorescent signal) and DAPI nuclear staining dye (350 nm excitation wavelength/460 nm emission filter for blue fluorescent signal) for 1 h at room temperature (RT). The fluorescent signal was observed under the fluorescence microscope.

2.8. Real-time PCR

The treated cells were subjected to RNA extraction using Trizol reagent. RNA was treated with DNase and converted to cDNA using a cDNA synthesis kit. Real-time PCR was performed using the Luna Universal qPCR Master Mix with the CFX96 touch real-time PCR detection system. The following primer sequences were used: *Mfn-1* Fw 5′-CTCCTTCTAACCCAGCAGCC, Rw 5′-GTTTTCCAAATCACGCCCCC, *Mfn-2* Fw 5′- CTCCATTCAAGAAGCTTGGACA, Rw 5′- CCTTCA-CAGGTTGGGCATCG, *OPA-1* Fw 5′- CAGTTTAGCTCCCGACCTGG, Rw 5′- CACCAAGCAGACCCTTCCTG, *Pink-1* Fw 5′- GTGGGACTCA-GATGGCTGTC, Rw 5′- CGCTCTACACTGGAGCTGTT, *Cyt-c* Fw 5′-AATCTCCACGGTCTGTTCGG, Rw 5′- GCACTGGTTAACCCAAGCAA and *GAPDH* Fw 5′-AGGTCGGTGTGAACGGATTTG, Rw 5′-TGTA-GACCATGTAGTTGAGGTCA. The relative gene expression was calculated using the $2^{-\Delta\Delta ct}$ method.

2.9. Western blotting

The treated cells were washed and subjected to protein extraction using a radioimmunoprecipitation assay buffer with a protease and phosphatase inhibitor cocktail. Equal amounts of proteins were separated by sodium dodecyl sulfate polyacrylamide gel electrophoresis and transferred into a polyvinylidene fluoride membrane. After blocking with goat serum at RT for 1 h, the membrane was incubated with the

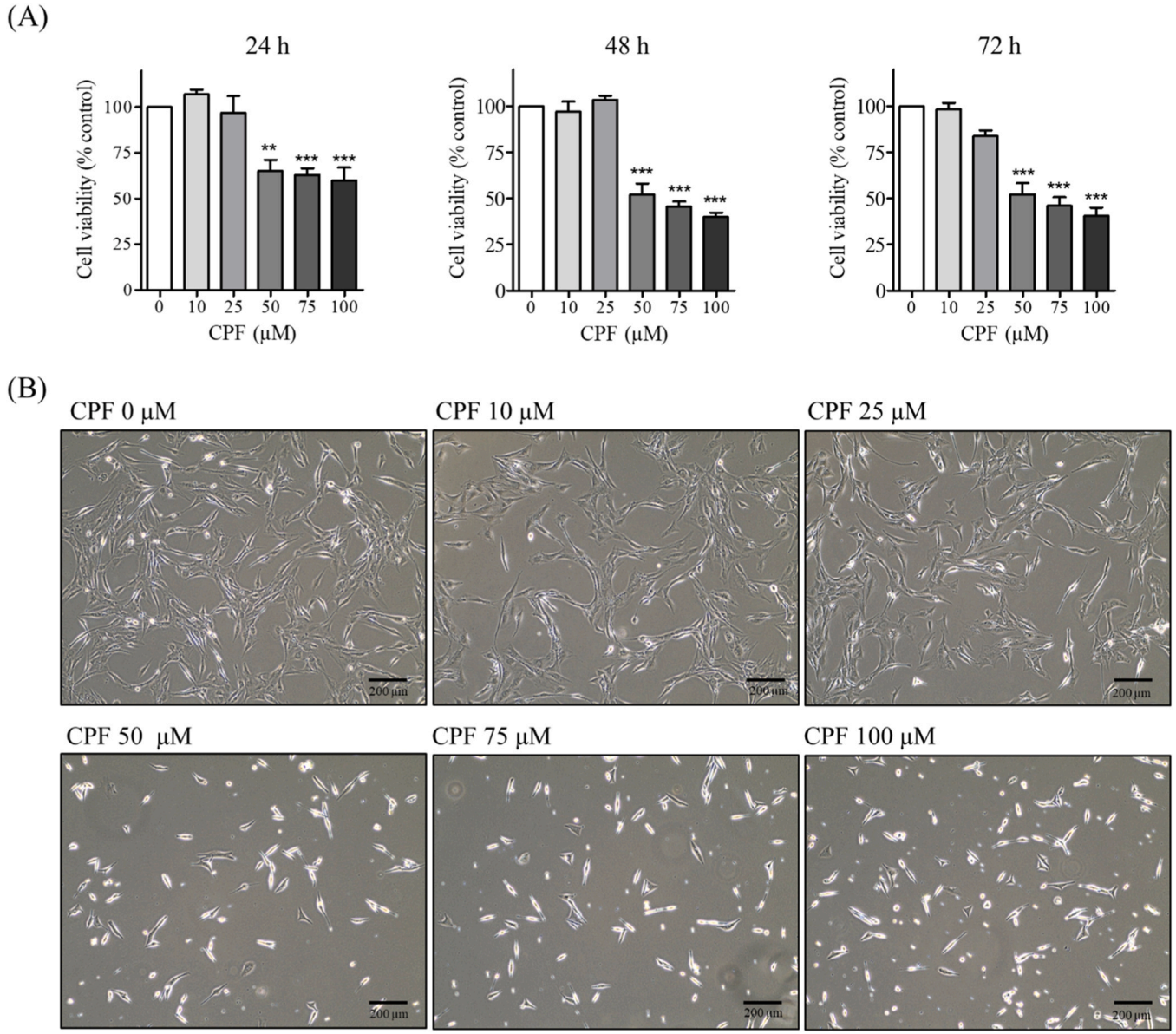

Fig. 2. Cytotoxicity of Chlorpyrifos (CPF) on C2C12 myoblast cells. Subconfluent C2C12 myoblasts were cultured in low-serum medium containing CPF at 0–100 μM for 24–72 h. Cell viability was determined by MTT assay (A) and cell morphology was photographed (B). $^{**}P < 0.01$, $^{***}P < 0.001$ compared with control. Scale bar = 200 μm.

desired primary antibody overnight at 4 °C. After several washes, the membrane was incubated with an appropriate secondary antibody conjugated with horseradish peroxidase. The protein signal was visualised using enhanced chemiluminescence under the Alliance Q9 advanced chemiluminescence imager (UVITEC, Cambridge, UK). The band intensity was measured using ImageJ software (version 1.8.0).

2.10. Statistical analysis

Data were presented as mean ± S.E.M. from at least three independent experiments. Statistical analysis was performed using the one-way analysis of variance (ANOVA) followed by a Tukey post hoc test. A Student's *t*-test was used to compare differences between two groups. *P*-

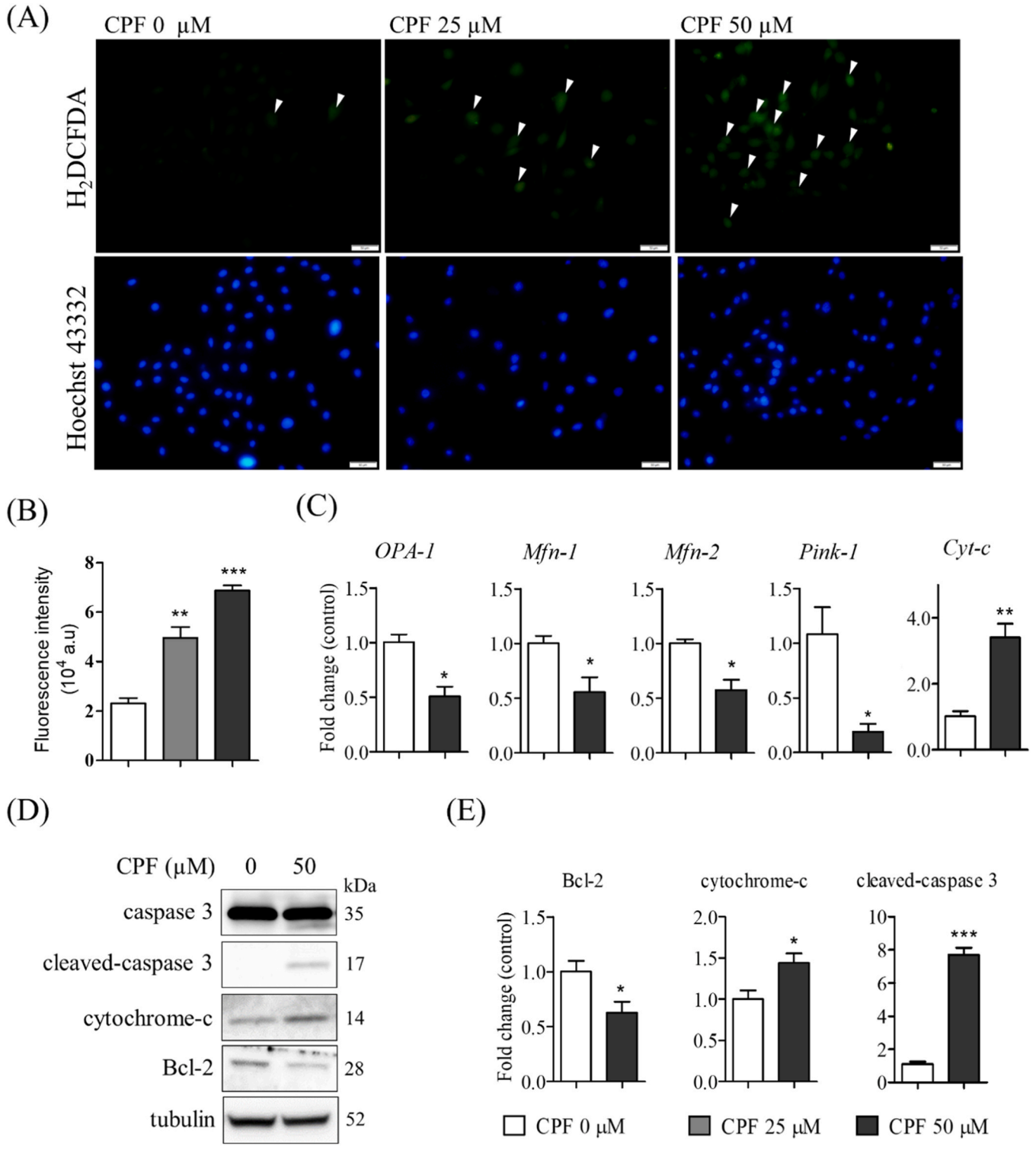

Fig. 3. Chlorpyrifos (CPF) stimulated reactive oxygen species (ROS) production. C2C12 myoblasts were cultured in CPF at indicated concentrations for 72 h. ROS production was observed by H_2DCFDA assay (green, arrowhead) (A) and fluorescence intensity was measured (B). Expression of mitochondrial-related genes was determined by real-time PCR (C). Expression of apoptotic markers was determined by western blotting (D) and band intensity was measured (E). $^{*}P < 0.05$, $^{**}P < 0.01$, $^{***}P < 0.001$ compared with control. Scale bar = 50 μm.

values < 0.05 were considered significant.

3. Results

3.1. Cytotoxicity of CPF in C2C12 myoblast cells

To examine the effect of CPF on C2C12 myoblast cell viability, the subconfluent myoblasts were cultured in media containing CPF at 0–100 μM for 24, 48, and 72 h. MTT results revealed that concentrations of 10–25 μM CPF were non-toxic to myoblasts throughout the 72 h. However, CPF at 50–100 μM significantly abrogated cell viability from 24 h (Fig. 2A). These findings were consistent with the phase contrast results in which control and 10–25 μM CPF treated groups showed comparable cell numbers and normal morphology with radial branching and long fibres extending in many directions. In contrast, myoblasts cultured in 50–100 μM CPF had low cell numbers, with most of the cells becoming round in shape and beginning to detach from the cell culture dish (Fig. 2B).

3.2. CPF triggered C2C12 myoblast stress

As toxic chemicals have been reported to cause cellular stress, this study evaluated the levels of ROS in myoblast cells following treatment with CPF. A H_2DCFDA assay showed accumulation of ROS in myoblasts after 48 h of exposure to CPF in a dose-dependent manner (Fig. 3A). Fluorescence intensity analysis revealed significant ROS increase in 25–50 μM CPF treated groups compared with the control group (Fig. 3B). In addition, real-time PCR showed significant changes in mitochondrial-related gene expression. Treatment with CPF significantly downregulated the expression of *Mfn-1*, *Mfn-2*, *OPA-1*, and *Pink-1*, and upregulated *Cyt-c* expression (Fig. 3C). Moreover, the expression of Bcl-2 protein was significantly decreased; the levels of Cyt-c and cleaved-caspase 3 proteins, markers for cellular apoptosis, were significantly increased (Fig. 3D and E).

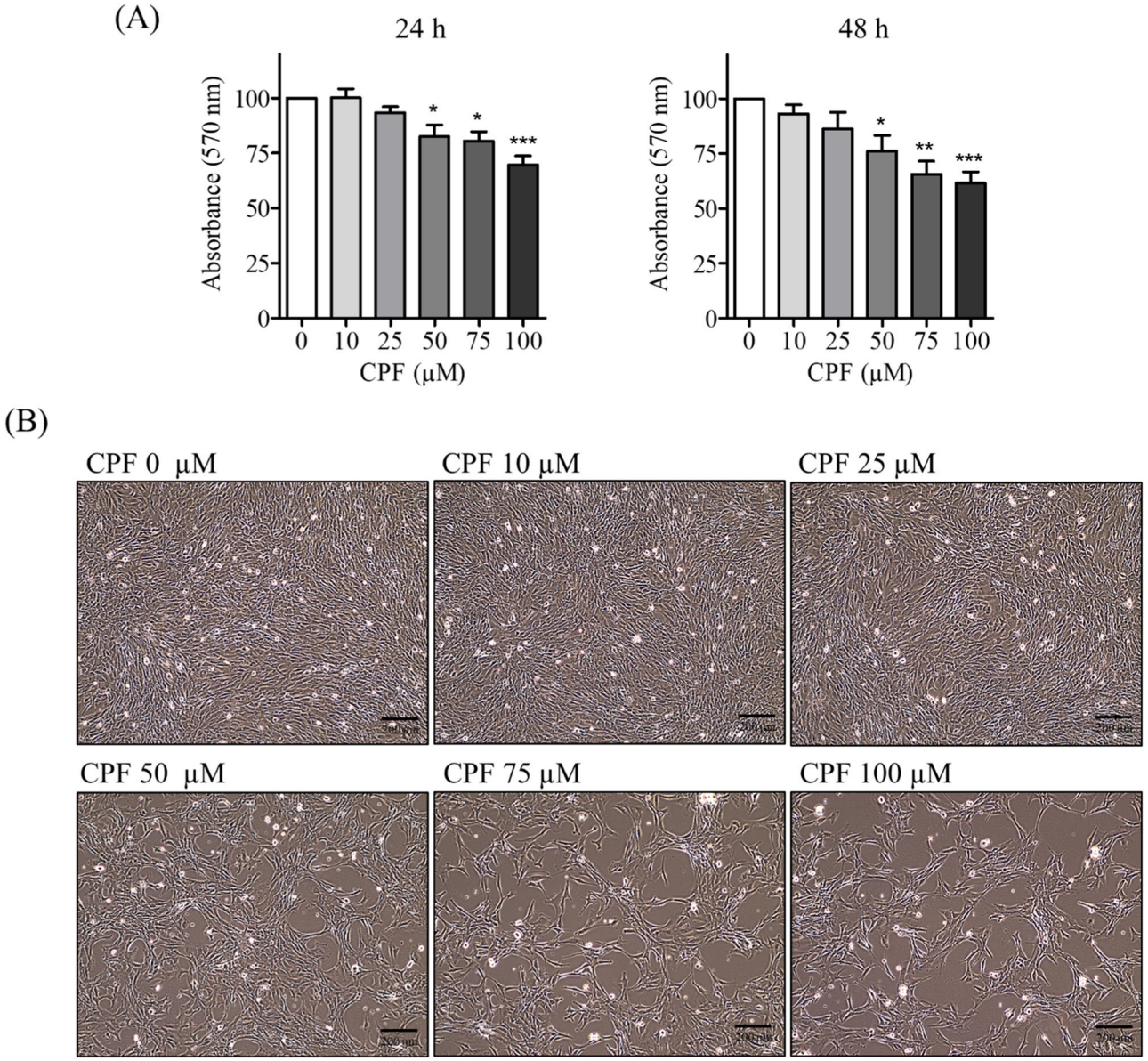

Fig. 4. Chlorpyrifos (CPF) inhibited C2C12 myoblast proliferation. Subconfluent C2C12 myoblasts were cultured in growth medium containing CPF at 0–100 μM for 24 and 48 h. Cell proliferation was determined by MTT assay (A) and cell morphology at 48 h after treatment was photographed (B). $^{*}P < 0.05$, $^{**}P < 0.01$, $^{***}P < 0.001$ compared with control. Scale bar = 200 μm.

3.3. CPF inhibited C2C12 myoblast proliferation

To investigate the effect of CPF on proliferation, myoblast cells were cultured in GM containing 10–100 μM CPF. MTT results showed that treatment with 50–100 μM CPF significantly inhibited myoblast cell proliferation from 24 h of exposure. The level of inhibition was both dose- and time-dependent (Fig. 4A). These results were consistent with the phase contrast images which revealed that cell confluence in the 50–100 μM CPF treatment groups was lower than the control group; however, 10–25 μM treated groups showed confluences comparable with the control group (Fig. 4B). While cell counting confirmed the significant decrease in cell numbers in CPF treated groups (Fig. 5A), Ki-67 immunostaining was considered positive (red, arrowhead) in most nuclei, meaning that they retained proliferation potential. However, the

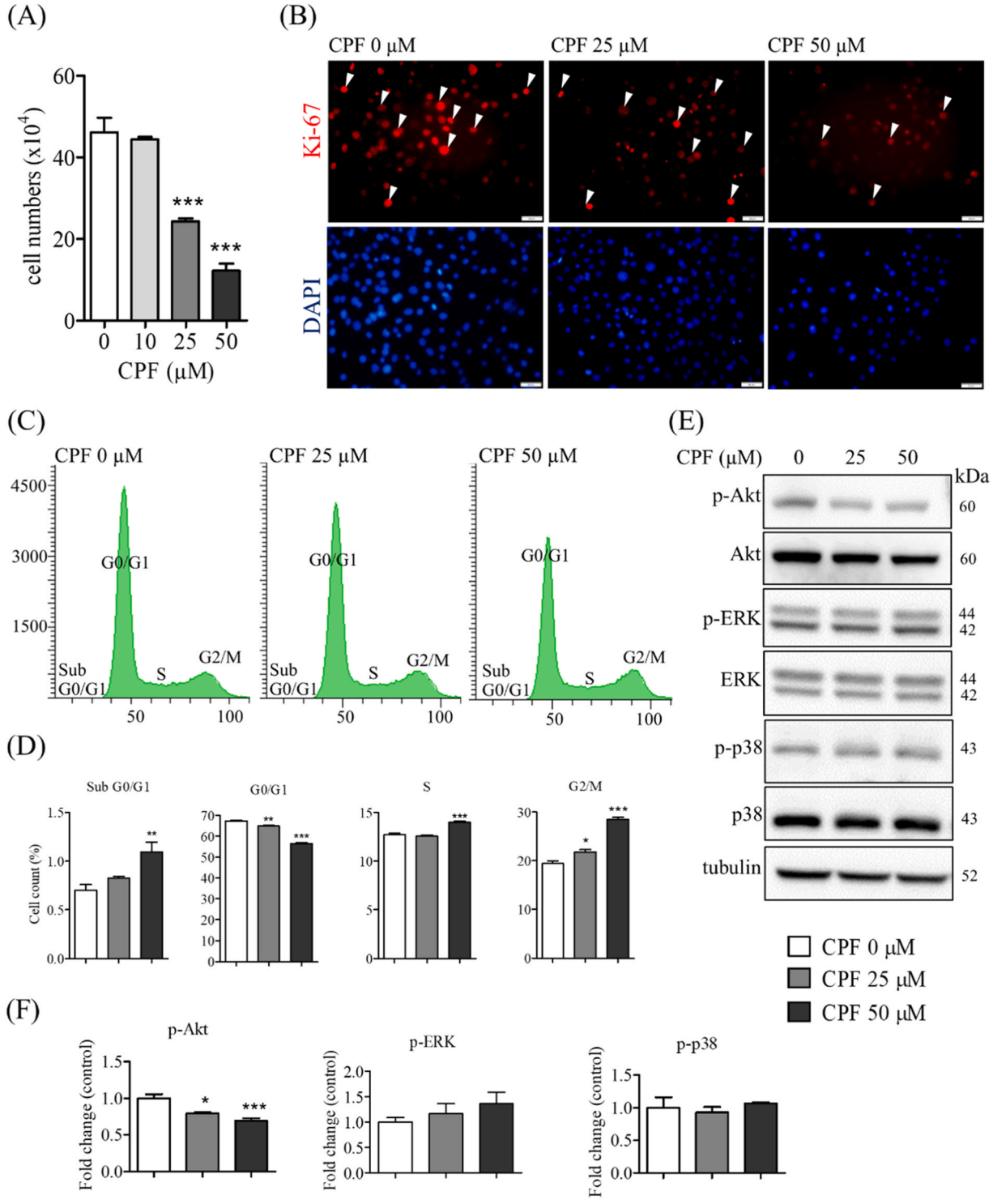

Fig. 5. Chlorpyrifos (CPF) stimulated myoblast cell cycle arrest. Subconfluent C2C12 myoblasts were cultured in growth medium containing CPF at indicated concentrations for 48 h. Cell proliferation was determined by cell counting (A) and Ki-67 immunostaining (red, arrowhead) (B). Cell cycle distribution was determined by flow cytometry (C) and percentage of cells at each stage was calculated (D). Protein expression was determined by western blotting (E) and band intensity was measured (F). $^{*}P < 0.05$, $^{**}P < 0.01$, $^{***}P < 0.001$ compared with control. Scale bar = 50 μm.

staining intensity of most nuclei in the control group was higher than in CPF treated groups (Fig. 5B). Flow cytometry analysis revealed a significant decrease in the number of cells at G0/G1, but an increased accumulation of cells in the Sub G0/G1, S, and G2/M cell cycle phases (Fig. 5C and D). To determine the possible mechanism of myoblast proliferation inhibition by CPF, several phosphorylated proteins were observed. CPF significantly decreased phosphorylated Akt, but not ERK and P38 MAPK (Fig. 5E and F).

3.4. CPF abrogated C2C12 myoblast differentiation

After 72 h in DM, myoblasts in the control group differentiated into multinucleated myotubes. Myoblasts cultured in DM with 10–25 μM CPF showed small numbers and sizes of myotubes (green, arrowhead) compared with the control group (Fig. 6A). CPF at 50–100 μM almost completely inhibited myoblast differentiation; only small and scant myotubes were present (data not shown). Myotube diameter measurements revealed that treatment with CPF significantly decreased diameter compared with the control group (Fig. 6B). Western blotting demonstrated that CPF significantly inhibited myoblast differentiation, as revealed by decreased MHC protein expression. The level of myogenin, an important myogenic regulatory factor for myoblast fusion, was also significantly decreased compared with the control group (Fig. 6C and D). Finally, treatment with CPF significantly decreased

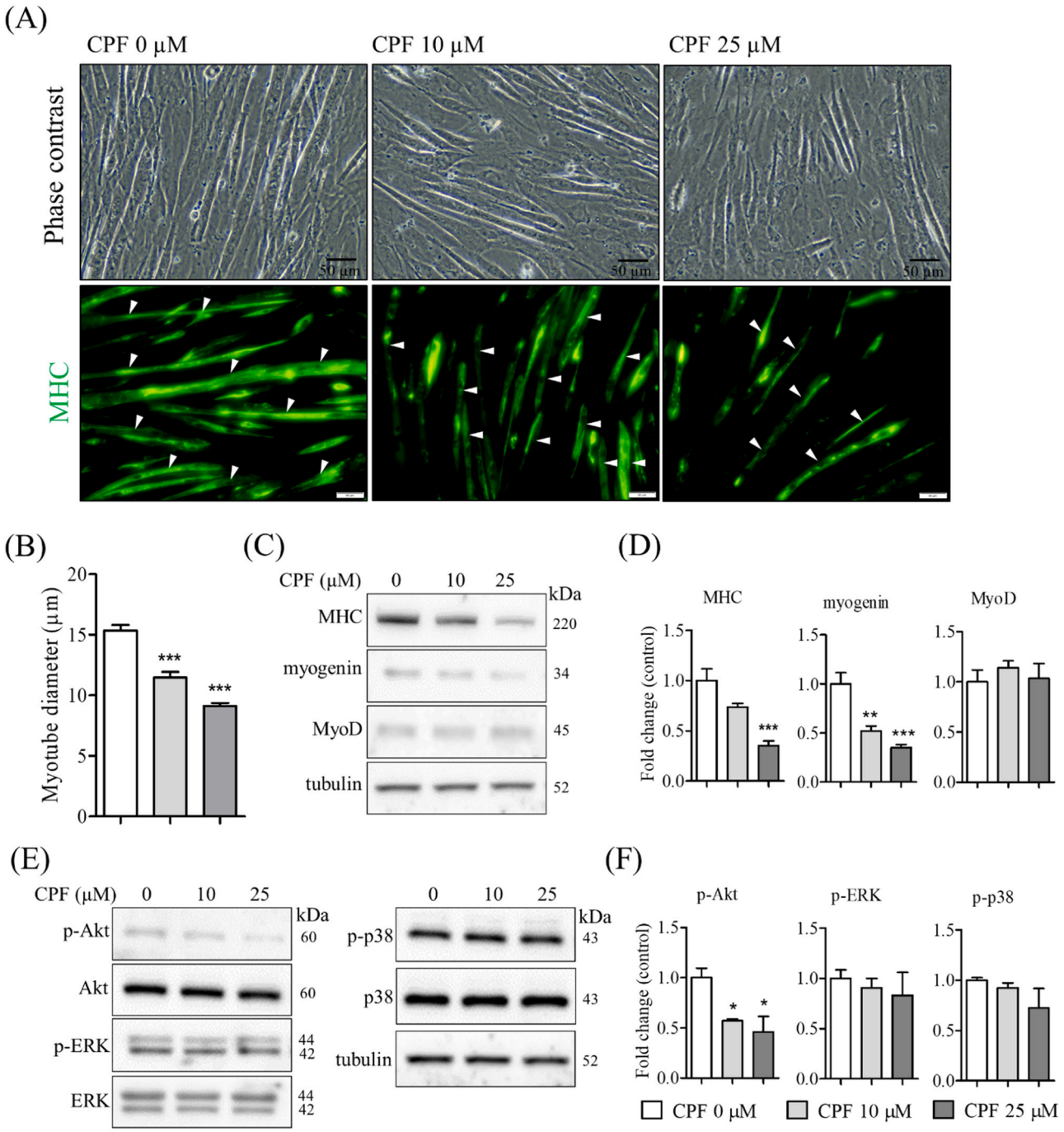

Fig. 6. Chlorpyrifos (CPF) abrogated C2C12 myoblast differentiation. Confluent C2C12 myoblasts were switched into differentiation medium containing CPF at 0–25 μM for 72 h. Myotubes were photographed and stained with anti-myosin heavy chain antibody (green, arrowhead) (A). Myotube size was measured (B). Protein expression was evaluated by western blotting (C, E) and band intensity was measured (D, F). *$P < 0.05$, **$P < 0.01$, ***$P < 0.001$. Scale bar = 50 μm.

phosphorylated Akt, but not ERK and p38 MAPK proteins (Fig. 6E and F).

4. Discussion

The present study is the first report on the adverse effects of CPF on C2C12 myoblast stress and myogenesis. The dosage of CPF which caused adverse effects (10–50 μM) was comparable with other toxic chemicals such as styrene oxide (25 μM) [14] and bisphenol-A (10–50 μM) [13]. C2C12 myoblasts exposed to toxic chemicals have been shown to decrease in viability and alter morphology, becoming round in shape and detaching from the culture dish [13,14,17]. A possible mechanism may occur via the decrease in antioxidant enzymes and the induction of mitochondrial stress, leading to cellular apoptosis [13,18]. Moreover, it has been reported that CPF exposure caused DNA damage and epigenetic alterations in liver cells, leading to various adverse effects [19].

Of interest, the current study revealed increases in ROS accumulation due to CPF treatment in a dose-dependent manner. It is well known that toxic substances cause cellular stress by inhibiting antioxidant enzymes, leading to ROS production and accumulation in various cell types [20]. CPF has also been reported to stimulate oxidative stress in neuronal cells and trigger neuronal cell death via apoptotic pathways [21], as well as cause stress and ROS accumulation in microglial cells [22], HepG2 cells [23], and mice cerebral and ocular tissue [24]. The increase in ROS causes cellular adverse effects, especially mitochondrial dysfunction and apoptosis induction [23].

The assessment of mitochondrial-related gene expression revealed expression modulation following CPF treatment. CPF suppressed Optic atrophy type 1 (*OPA-1*), Mitofusin 1 (*Mfn-1*), and Mitofusin 2 (*Mfn-2*) genes, which are responsible for mitochondrial biogenesis by regulating mitochondrial fission and fusion kinetics. Balancing fission and fusion is important in maintaining a healthy mitochondrial population via mitophagy [25,26]. Disrupting the fusion–fission equilibrium increases mitochondrial fragmentation and accumulation of defective mitochondria, leading to dysfunction and cellular apoptosis [26]. ROS accumulation has also been reported to modulate the expression of PTEN-induced putative kinase 1 (*Pink-1*), which protects mitochondria from cellular stress, regulates mitophagy, and works with Parkin protein to maintain mitochondrial function. Increase in oxidative stress has been shown to modulate *Pink-1* expression [27]. Pink-1 protects against cell death by inhibiting autophagy through phosphorylating Bcl-xL and impairing its pro-apoptotic cleavage [28]. Exposure to toxic chemicals downregulates the expression of *Pink-1*; the knockdown of *Pink-1* reduces cell proliferation and increases apoptosis [29]. Mitochondrial disruption is known to be a key mediator of the intrinsic apoptosis pathway. This study showed CPF-induced intrinsic apoptosis via the upregulation of cytochrome c (*Cyt-c*) expression. Cytochrome c plays an important role in apoptosis by binding with Apf-1 to form apoptosome, ultimately resulting in caspase activation and DNA fragmentation [30]. Moreover, the decrease in Bcl-2 protein causes cytochrome c efflux from mitochondria, resulting in caspase-3 activation. However, to gain insight into the effect of CPF on mitochondrial stress, future investigations measuring antioxidant enzymatic activity and other apoptotic-related gene and protein expressions are required.

CPF has been shown to inhibit cell proliferation in 3T3-L1 [31], breast cancer [32], and human neuroblastoma SH-SY5Y [33] cells via different mechanisms. This is consistent with previous studies in which myoblast cells exposed to toxic chemicals showed proliferation inhibition and cell cycle arrest at S and G2/M phases [13,14]. The major cause of antiproliferation in chemical exposure conditions has been suggested as the increase in ROS and cellular stress [14,29]. ROS increase has been reported to mediate inactivation of the PI3K/Akt pathway [34] which plays an important role in cell proliferation by enhancing cyclin-D1 and PCNA expression [35,36]. Inhibition of Akt has been shown to inhibit cell proliferation and induce apoptosis [37].

Regarding myoblast differentiation, these results are consistent with previous studies demonstrating that high-phosphate chemicals suppressed myoblast differentiation by increasing cellular stress [38]. This suppression has been reported to reduce MHC and other myogenic regulatory protein expression, as well as reduce both the number and size of multinucleated myotubes [13,14]. CPF has also been shown to affect the contractility and the expression isoforms of diaphragm muscle in rats [10]. As phosphorylated Akt is upstream of myogenin in myoblast differentiation [39], its suppression may lead to a decrease in myogenin expression and ultimately abrogate myoblast differentiation. Both MyoD and myogenin proteins are necessary factors for myoblast fusion during myogenesis [12,19]. The knockdown of myogenin has been shown to reduce the fusion of myoblasts into multinucleated myotubes [40]. These confirm that CPF abrogates myogenic differentiation by suppressing phosphorylated Akt protein expression.

5. Conclusions

This is the first study on the adverse effects of CPF on skeletal muscle development and regeneration. These results demonstrated the dose-dependent cytotoxicity and mitochondrial stress in myoblasts exposed to CPF. CPF exposure increased intracellular ROS and modulated the expression of mitochondrial-related genes, giving rise to apoptosis. Moreover, it inhibited myoblast cell proliferation by stimulating cell accumulation at SubG0/G1, S, and G2/M cell cycle phases, and diminished myoblast differentiation. One possible mechanism occurs through the suppression of phosphorylated Akt protein. These findings raise concerns about the potential adverse effects of CPF contamination in agricultural products on consumers.

CRediT authorship contribution statement

Tipbunjong Chittipong: Writing – review & editing, Writing – original draft, Visualization, Validation, Supervision, Software, Resources, Project administration, Methodology, Investigation, Funding acquisition, Formal analysis, Data curation, Conceptualization. **Hengpratom Tanaporn:** Writing – review & editing, Writing – original draft, Visualization, Data curation. **Thitiphatphuvanon Thanvarin:** Writing – review & editing, Writing – original draft, Visualization, Investigation, Data curation. **Bunnuang Kornkanok:** Investigation, Data curation. **Watthanard Mariam:** Resources, Data curation. **Salika Thanaporn:** Visualization, Investigation, Data curation. **Jiraarpassorn Chatchakwan:** Visualization, Investigation, Data curation. **Petmunee Laksika:** Visualization, Investigation, Formal analysis, Data curation. **Surinlert Piyaporn:** Writing – review & editing, Writing – original draft, Visualization, Software, Resources, Investigation, Funding acquisition, Formal analysis, Data curation, Conceptualization.

Declaration of Competing Interest

The authors declare that they have no known competing financial interests or personal relationships that could have appeared to influence the work reported in this paper.

Acknowledgements

This research was supported by the Faculty of Science Research Fund (2019), Prince of Songkla University, and partially supported by the Thailand Science Research and Innovation (TSRI) Fundamental Fund, fiscal year 2025, Thammasat University.

Data availability

Data will be made available on request.

References

[1] R.C. Gilden, K. Huffling, B. Sattler, Pesticides and health risks, J. Obstet. Gynecol. Neonatal Nurs. 39 (1) (2010) 103–110, https://doi.org/10.1111/j.1552-6909.2009.01092.

[2] J. Hitchmough, Environmental horticulture science and management of green landscapes, CABI, Oxfordshire, UK, 2016.

[3] A. Rathod, R. Garg, Chlorpyrifos poisoning and its implications in human fatal cases: a forensic perspective with reference to Indian scenario, J. Forensic Leg. Med 47 (2017), https://doi.org/10.1016/j.jflm.2017.02.003.

[4] C. Timchalk, R.J. Nolan, A.L. Mendrala, D.A. Dittenber, K.A. Brzak, J.L. Mattsson, A physiologically based pharmacokinetic and pharmacodynamic (PBPK/PD) model for the organophosphate insecticide chlorpyrifos in rats and humans, Toxicol. Sci. 66 (1) (2002) 34–53, https://doi.org/10.1093/toxsci/66.1.34.

[5] T.J. Cook, S.S. Shenoy, Intestinal permeability of chlorpyrifos using the single-pass intestinal perfusion method in the rat, Toxicology 184 (2-3) (2003) 125–133, https://doi.org/10.1016/s0300-483x(02)00555-3.

[6] L.A. Geer, N. Cardello, M.J. Dellarco, T.J. Leighton, R.P. Zendzian, J.D. Roberts, T. J. Buckley, Comparative analysis of passive dosimetry and biomonitoring for assessing chlorpyrifos exposure in pesticide workers, Ann. Occup. Hyg. 48 (8) (2004) 683–695, https://doi.org/10.1093/annhyg/meh056.

[7] W.J.A. Meuling, L.C. Ravensberg, L. Roza, J.J.V. Hemmen, Dermal absorption of chlorpyrifos in human volunteers, Int Arch. Occup. Environ. Health 78 (1) (2005) 44–50, https://doi.org/10.1007/s00420-004-0558-6.

[8] D.T. Mage, Dermal absorption of Chlorpyrifos, Ann. Occup. Hyg. 50 (6) (2006) 638–639, https://doi.org/10.1093/annhyg/mel037.

[9] L. Schulze, C. Ogg, E. Vitzthum, EC97-2505 Signs symptoms Pestic. Poison (1997).

[10] H.E.K. El Sabbouri, N. Hallal, W. Darwiche, J. Gay-Quéheillard, V. Bach, W. Ramadan, W.H. Joumaa, Effect of chronic chlorpyrifos exposure on diaphragmatic muscle contractility and MHC isoforms in adult rats, Toxicol. Environ. Health Sci. 14 (1) (2022) 77–87, https://doi.org/10.1007/s13530-021-00121-6.

[11] F. Le Grand, M.A. Rudnicki, Skeletal muscle satellite cells and adult myogenesis, Curr. Opin. Cell Biol. 19 (6) (2007) 628–633, https://doi.org/10.1016/j.ceb.2007.09.012.

[12] S. Grefte, A.M. Kuijpers-Jagtman, R. Torensma, J.W. Von den Hoff, Skeletal muscle development and regeneration, Stem Cells Dev. 16 (5) (2007) 857–868, https://doi.org/10.1089/scd.2007.0058.

[13] C. Tipbunjong, T. Thitiphatphuvanon, C. Pholpramool, P. Surinlert, Bisphenol-A abrogates proliferation and differentiation of C2C12 mouse myoblasts via downregulation of phospho-P65 NF-κB signaling pathway, J. Toxicol. 2024 (2024) 3840950, https://doi.org/10.1155/2024/3840950.

[14] P. Surinlert, N. Kongthong, M. Watthanard, T. Sae-Lao, P. Sookbangnop, C. Pholpramool, C. Tipbunjong, Styrene oxide caused cell cycle arrest and abolished myogenic differentiation of C2C12 myoblasts, J. Toxicol. 2020 (2020) 1807126, https://doi.org/10.1155/2020/1807126.

[15] Y.P. Yen, K.S. Tsai, Y.W. Chen, C.F. Huang, R.S. Yang, S.H. Liu, Arsenic inhibits myogenic differentiation and muscle regeneration, Environ. Health Perspect. 118 (7) (2010) 949–956, https://doi.org/10.1289/ehp.0901525.

[16] K. Akiyama, J. Tone, M. Okabe, S. Nishimoto, T. Sugahara, Y. Kakinuma, Inhibition of myotube formation by paraquat in the myoblast cell line C2C12, J. Toxicol. Sci. 36 (2) (2011) 243–246, https://doi.org/10.2131/jts.36.243.

[17] A. Ordóñez-Vásquez, L. Jaramillo-Gómez, C. Duran-Correa, E. Escamilla-García, M. A. De la Garza-Ramos, F. Suárez-Obando, A reliable and reproducible model for assessing the effect of different concentrations of α-Solanine on rat bone marrow mesenchymal stem cells, Bone Marrow Res 2017 (2017) 2170306, https://doi.org/10.1155/2017/2170306.

[18] K. Niaz, F. Mabqool, F. Khan, F. Ismail Hassan, M. Baeeri, M. Navaei-Nigjeh, S. Hassani, M. Gholami, M. Abdollahi, Molecular mechanisms of action of styrene toxicity in blood plasma and liver, Environ. Toxicol. 32 (10) (2017) 2256–2266, https://doi.org/10.1002/tox.22441.

[19] P. Balakrishnan, K. Thirunavukarasu, P. Tamizhmani, A.A. Michael, T. Velusamy, Toxicological Impact of chronic chlorpyrifos exposure: DNA damage and epigenetic alterations induces neoplastic transformation of liver cells, Biochem Biophys. Res Commun. 746 (2025) 151287, https://doi.org/10.1016/j.bbrc.2025.151287.

[20] M. Wójciak, P. Drozdowski, A. Ziemlewska, M. Zagórska-Dziok, Z. Nizioł-Łukaszewska, T. Kubrak, I. Sowa, ROS scavenging effect of selected isoflavones in provoked oxidative stress conditions in human skin fibroblasts and keratinocytes, Molecules 29 (5) (2024) 955.

[21] J.W. Lin, S.C. Fu, J.M. Liu, S.H. Liu, K.I. Lee, K.M. Fang, R.J. Hsu, C.F. Huang, K. M. Liu, K.C. Chang, C.C. Su, Y.W. Chen, Chlorpyrifos induces neuronal cell death via both oxidative stress and Akt activation downstream-regulated CHOP-triggered apoptotic pathways, Toxicol. Vitr. 86 (2023) 105483, https://doi.org/10.1016/j.tiv.2022.105483.

[22] G.C.C. Weis, C.E. Assmann, V.B. Mostardeiro, A.O. Alves, J.R. da Rosa, M.M. Pillat, C.M. de Andrade, M.R.C. Schetinger, V.M.M. Morsch, I.B.M. da Cruz, I. H. Costabeber, Chlorpyrifos pesticide promotes oxidative stress and increases inflammatory states in BV-2 microglial cells: a role in neuroinflammation, Chemosphere 278 (2021) 130417, https://doi.org/10.1016/j.chemosphere.2021.130417.

[23] C. Montanarí, F. Franco-Campos, M. Taroncher, Y. Rodríguez-Carrasco, V. Zingales, M.J. Ruiz, Chlorpyrifos induces cytotoxicity via oxidative stress and mitochondrial dysfunction in HepG2 cells, Food Chem. Toxicol. 192 (2024) 114933, https://doi.org/10.1016/j.fct.2024.114933.

[24] A.A. AlKahtane, E. Ghanem, S.G. Bungau, S. Alarifi, D. Ali, G. AlBasher, S. Alkahtani, L. Aleya, M.M. Abdel-Daim, Carnosic acid alleviates chlorpyrifos-induced oxidative stress and inflammation in mice cerebral and ocular tissues, Environ. Sci. Pollut. Res Int 27 (11) (2020) 11663–11670, https://doi.org/10.1007/s11356-020-07736-1.

[25] C. Vantaggiato, M. Castelli, M. Giovarelli, G. Orso, M.T. Bassi, E. Clementi, C. De Palma, The fine tuning of Drp1-dependent mitochondrial remodeling and autophagy controls neuronal differentiation, Front Cell Neurosci. 13 (2019) 120, https://doi.org/10.3389/fncel.2019.00120.

[26] D. Nayak, D. Adiga, N.G. Khan, P.S. Rai, H.S. Dsouza, S. Chakrabarty, N. R. Gassman, S.P. Kabekkodu, Impact of bisphenol A on structure and function of mitochondria: a critical review, Rev. Environ. Contam. Toxicol. 260 (1) (2022) 10, https://doi.org/10.1007/s44169-022-00011-z.

[27] S.K. Barodia, R.B. Creed, M.S. Goldberg, Parkin and PINK1 functions in oxidative stress and neurodegeneration, Brain Res Bull. 133 (2017) 51–59, https://doi.org/10.1016/j.brainresbull.2016.12.004.

[28] G. Arena, V. Gelmetti, L. Torosantucci, D. Vignone, G. Lamorte, P. De Rosa, E. Cilia, E.A. Jonas, E.M. Valente, PINK1 protects against cell death induced by mitochondrial depolarization, by phosphorylating Bcl-xL and impairing its pro-apoptotic cleavage, Cell Death Differ. 20 (7) (2013) 920–930, https://doi.org/10.1038/cdd.2013.19.

[29] Z. Si, Z. Shen, F. Luan, J. Yan, PINK1 regulates apoptosis of osteosarcoma as the target gene of cisplatin, J. Orthop. Surg. Res. 18 (1) (2023) 132, https://doi.org/10.1186/s13018-023-03615-w.

[30] M. Mustafa, R. Ahmad, I.Q. Tantry, W. Ahmad, S. Siddiqui, M. Alam, K. Abbas, M. I. Moinuddin, S. Hassan, S. Habib, Apoptosis: a comprehensive overview of signaling pathways, morphological changes, and physiological significance and therapeutic implications, Cells 13 (22) (2024) 1838.

[31] M. Czajka, K. Sawicki, M. Matysiak-Kucharek, M. Kruszewski, J. Kurzepa, P. Wojtyła-Buciora, L. Kapka-Skrzypczak, Exposure to chlorpyrifos alters proliferation, differentiation and fatty acid uptake in 3T3-L1 cells, Int J. Mol. Sci. 24 (22) (2023), https://doi.org/10.3390/ijms242216038.

[32] C. Ventura, A. Venturino, N. Miret, A. Randi, E. Rivera, M. Núñez, C. Cocca, Chlorpyrifos inhibits cell proliferation through ERK1/2 phosphorylation in breast cancer cell lines, Chemosphere 120 (2015) 343–350, https://doi.org/10.1016/j.chemosphere.2014.07.088.

[33] M.W. Zhao, P. Yang, L.L. Zhao, Chlorpyrifos activates cell pyroptosis and increases susceptibility on oxidative stress-induced toxicity by miR-181/SIRT1/PGC-1α/Nrf2 signaling pathway in human neuroblastoma SH-SY5Y cells: implication for association between chlorpyrifos and Parkinson's disease, Environ. Toxicol. 34 (6) (2019) 699–707, https://doi.org/10.1002/tox.22736.

[34] C. Wen, H. Wang, X. Wu, L. He, Q. Zhou, F. Wang, S. Chen, L. Huang, J. Chen, H. Wang, W. Ye, W. Li, X. Yang, H. Liu, J. Peng, ROS-mediated inactivation of the PI3K/AKT pathway is involved in the antigastric cancer effects of thioredoxin reductase-1 inhibitor chaetocin, Cell Death Dis. 10 (11) (2019) 809, https://doi.org/10.1038/s41419-019-2035-x.

[35] I. Kunter, E. Erdal, D. Nart, F. Yilmaz, S. Karademir, O. Sagol, N. Atabey, Active form of AKT controls cell proliferation and response to apoptosis in hepatocellular carcinoma, Oncol. Rep. 31 (2) (2014) 573–580, https://doi.org/10.3892/or.2013.2932.

[36] D. Ding, Z. Liu, L. Zhao, H. Geng, Z. Liang, D. Yu, Role of PI3K/Akt pathway in Benzidine-induced proliferation in SV-40 immortalized human uroepithelial cell, Transl. Cancer Res 8 (4) (2019) 1301–1310, https://doi.org/10.21037/tcr.2019.07.14.

[37] M. Mandal, M. Younes, E.A. Swan, S.A. Jasser, D. Doan, O. Yigitbasi, A. McMurphey, J. Ludwick, A.K. El-Naggar, C. Bucana, G.B. Mills, J.N. Myers, The Akt inhibitor KP372-1 inhibits proliferation and induces apoptosis and anoikis in squamous cell carcinoma of the head and neck, Oral. Oncol. 42 (4) (2006) 430–439, https://doi.org/10.1016/j.oraloncology.2005.09.011.

[38] L.H. Chung, S.T. Liu, S.M. Huang, D.M. Salter, H.S. Lee, Y.J. Hsu, High phosphate induces skeletal muscle atrophy and suppresses myogenic differentiation by increasing oxidative stress and activating Nrf2 signaling, Aging 12 (21) (2020) 21446–21468, https://doi.org/10.18632/aging.103896.

[39] C. Tipbunjong, P. Khuituan, Y. Kitiyanant, A. Suksamrarn, C. Pholpramool, Diarylheptanoid 1-(4-hydroxyphenyl)-7-phenyl-(6*E*)-6-hepten-3-one enhances C2C12 myoblast differentiation by targeting membrane estrogen receptors and activates Akt-mTOR and p38 MAPK-NF-κB signaling axes, J. Nat. Med 73 (4) (2019) 735–744, https://doi.org/10.1007/s11418-019-01322-7.

[40] E.J. Lee, A. Malik, S. Pokharel, S. Ahmad, B.A. Mir, K.H. Cho, J. Kim, J.C. Kong, D. M. Lee, K.Y. Chung, S.H. Kim, I. Choi, Identification of genes differentially expressed in myogenin knock-down bovine muscle satellite cells during differentiation through RNA sequencing analysis, PLoS One 9 (3) (2014) e92447, https://doi.org/10.1371/journal.pone.0092447.